CHAPTER 2

LITERATURE REVIEW

2.1 Introduction

The spur dykes are typically manufactured hydraulic structures that are protruded laterally from the bank into the river. In general, these structures are used as river training structures all around the world. The primary function of a spur dyke is to prevent bank erosion by diverting away from the main currents in rivers (Duan, 2009). The spur dyke resists the flow, which ensures the deepening of the main channel.

This study would examine the effect of spur dyke or related structures constructed on the natural channels attracting the attention of various researchers over several decades. Various studies were carried out to understand the flow characteristics, sediment transport, bed topography, scour, and morphologies around such shape. (Rajaratnam et al., 1983; Melville, 1992; Kwan et al., 1994; Kothyari et al., 2001; Singh et al., 2020); researchers have significantly contributed to this field. It should be noted that the majority of these studies have been performed in a straight channel. A brief review was written by Zhang, and Nakagawa, (2008); Pandey et al., (2018). Studies of this region have shown a recent shift towards the Spur dyke at the outer edge of the channel bend (curved channel). This review may provide the readers and scientists with up-to-date knowledge and findings of the studies carried out for the spur dyke situated at the channel bend. This chapter describes the flow characteristics near around spur dyke. The discussion then shifts to the spur dyke situated at the channel bend. It explicitly discusses the factors affecting the scour geometry. The formulations available in the

literature to estimate the scour geometry are discussed along with their validation using the experimental data from various other pieces of literature. It is further continued with elaborate findings on flow characteristics or patterns and bed topography (elevation) near around the spur dyke placed in the bend. In the end, numerical investigations, development, and findings in the related field are briefly discussed.

2.2 Flow pattern around a spur dyke – a general review

Spur dyke in river channel restricts natural flow, causing rapid flow area, which eventually influences sediment transportation and bed topography. In case when a dyke is present at the bend, these processes get further complicated. The flow near the spur dyke is highly responsible for the local scour, which further escalates with increasing scour depth. Therefore, it becomes crucial to understand the behaviour of the flow process near around a spur dyke.

Generally, the flow near the spur dyke can be further divided into three-zones, main flow zone, wake-up zone, and between this mixing zone. The main flow area extends from the top edge of the structure to the opposite side of the channel; the region extends from the bank from which the dyke is protruded to the head of the dyke is termed as the wake-up zone, and the mixing zone lies in the middle of two.

The main flow zone is characterized by an increase in flow velocity as compared to approaching flow velocity. This increment might be as much as 1.5 times incoming flow which depends on flow condition and the length of spur dyke to channel width ratio (Molinas et al., 1998). The wake zone consists of two sub-zones: a return and reattachment flow zone. Return flow zone may be defined as small eddies located near the spur dyke and a large eddy located farther from the spur dyke downstream. For the straight channel, various researchers reported the location of the centres of these eddies. Near the spur dyke, the stream flow gets separated from the channel bank from which the

spur dyke protrudes and gets reattached to the bank later downstream. The place at which the reattachment formed is called the reattachment zone. Various researchers (e. g. Fei et al., 1997; Yazdi et al., 2010; Zhang, and Nakagawa, 2008) carried out many experimental and numerical investigations for different types of spur dykes for the location and length of this zone. For instance, in an experiment conducted by Fei et. al., (1997), in a straight reach of the channel, reported that the length of the reattachment zone is approx 6 times the length of the dyke. Yazdi et al., (2010), mathematically investigated the flow characteristics near the inclined spur dyke and reported that the dimension of the reattachment zone for various inclinations remains nearly constant.

They also observed that the reattachment length affects the length of the spur dyke but remains unchanged irrespective of approaching flow discharge condition. Zhang, and Nakagawa, (2008), discuss the effect of permittivity and inclination of spur dykes on flow repetition and separation length.

Blockage of water flow due to the impact of spur dyke is influenced pressure distribution around the structure; due to this pressure gradient, there is a formation of 3D complex flow characteristics such as the generation of eddies, rollers, submerged vortices, and so on (Ettema et. al., 2004). At upstream of spur dyke, the water surface is characterized by the formation of the bow wave and a downflow. The stagnation of the flow causes this approach. At downstream of the structure, a system of wake vortices forms. Due to flow separation, horse-shoe vortices are formed in scour holes.

The flow pattern gets further complicated when the spur dyke was situated at the outer bank of the curved channel shown in Figure 2.1. This complexity is caused by the addition of some centrifugal force of the flow.

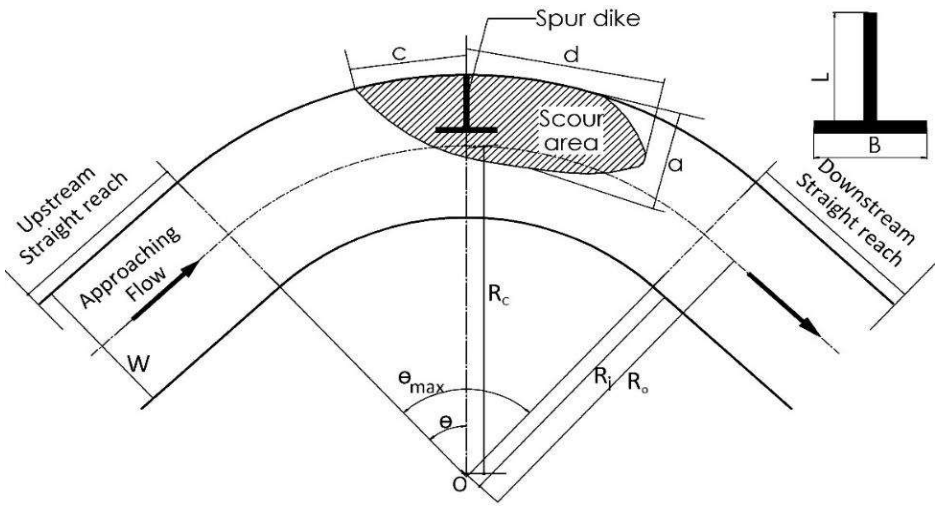

Figure 2.1 Typical plan views of a channel bend.

It results in the continuous change in flow momentum, which increases the erosion of the outer bank leading to its lateral migration. In past decay, the flow characteristics in the channel bend are studied by many of the researchers such as Shukry, (1950); Kikkawa et al., (1976); Odgaard et al., (1988); Giri et al., (2003), and so on. (Fazli et al., 2008) observed the flow field at 90° bend channel in the absence of a straight spur. The maximum local velocity position gradually shifted towards the inner bank, where the bend entered the outer bank at the exit. Rozovski (1957) reached a similar conclusion.

The flow field in such a case is associated with the complex flow like primary vortices, secondary flow, separation of flow, the rise of flow, and many more. Fazli et al., (2008) observed the typical and distinct flow behaviour around the spur dyke placed at various locations at 90° channel bend. While observing velocity of flow contour near the most water surface in the 90° bends, they further reported that the width of flow separation reduces towards the downstream when spur dyke is located near the entry of channel, i.e., θ = 30°. In contrast, the reverse is observed when located near the exit, i.e., θ = 75°. Here, θ is the angle of the dyke, which is measured by the penetration of the bend, as shown in Figure 2.2.

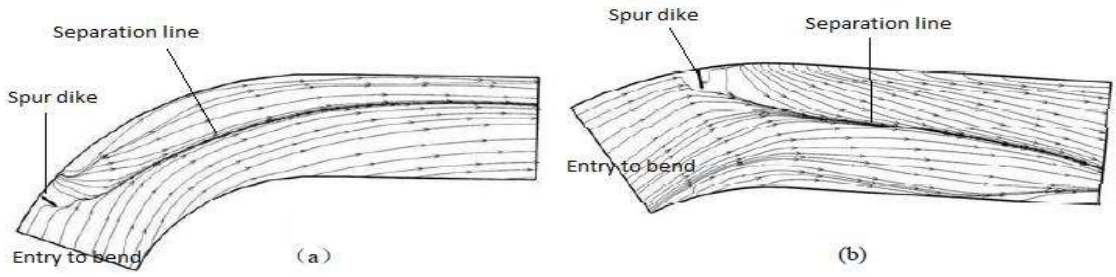

Figure 2.2 Flow contour near the water surface in 90° bend with spur dyke located at (a) 30° and (b) 75° (Fazli et al., 2008)

In short, with increasing distance of the spur dyke from the entrance of the bend, the separation area increases. Fazli et al., (2008) reported that all cross-sections upstream of the dyke are characterized by the up-flow vortices near the inner edge, which cause degradation at the upstream that sometimes extends to the downstream. Furthermore, they observed that the up-flow vortices were forming in the downstream spur dyke, which increases the location of the dyke shifted towards the exit of the bend. This up-flow vortex causes radial repelling of stream flow downstream of the spur dyke. Ghodsian et al., (2009) observed a similar phenomenon for formation of two types of vortices in the upstream of spur dike. In which the up-flow vortices close to the water surface and down flow vortices formed near the channel bed, revolving in clockwise and anti-clockwise manner respectively, and cross over the wing of structure (nose of spur dyke) as horizontal vortices (represented by (a) and (b) shown in Figure 2.2. These behaviours are caused because of the wing component of the spur dyke. In addition, they also observed some counter-clockwise vortices generated on the curved surface of scour hole and vertical vortices downstream of a spur dyke represented by (c) and (d) shown in Figure 2.3 respectively. By increasing the length of the dyke and stagnations zone, the protected area increased automatically.

This is due to reducing the helical flow and secondary flow. For the T-shaped spur dyke in a 90° bend, Vaghefi et al., (2017a) observed lateral flow formation upstream and

downstream of the spur dyke wing. The flow downstream is further associated with the formation of the main secondary flow. It was noticed that the secondary flows form along the inner bank, near the water surface at section 30^0 and continue to exist up to section 65^0, weakening and diminishing.

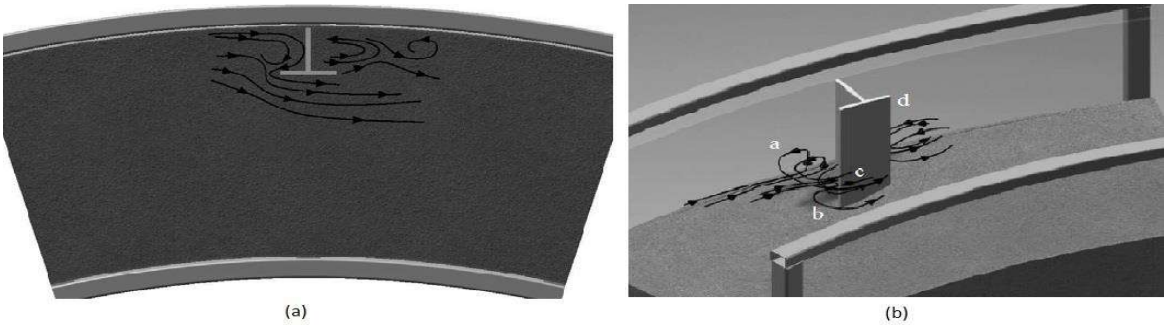

Figure 2.3 Vortices formed around T-shaped spur Dyke located at θ = 45° in the 90°channel (Ghodsian et al., 2009)

It concluded that the strength of secondary flow and vorticity can be high up with an increase in distance from the entry of bend up to section 74^0, decreasing between section 74^0 and 82.5^0. After that, these values increase up to the end of the bend. Potential variation in secondary flow and vorticity for a T-shaped spur located at an angle of $\theta = 75^0$ is shown in Figure 2.4.

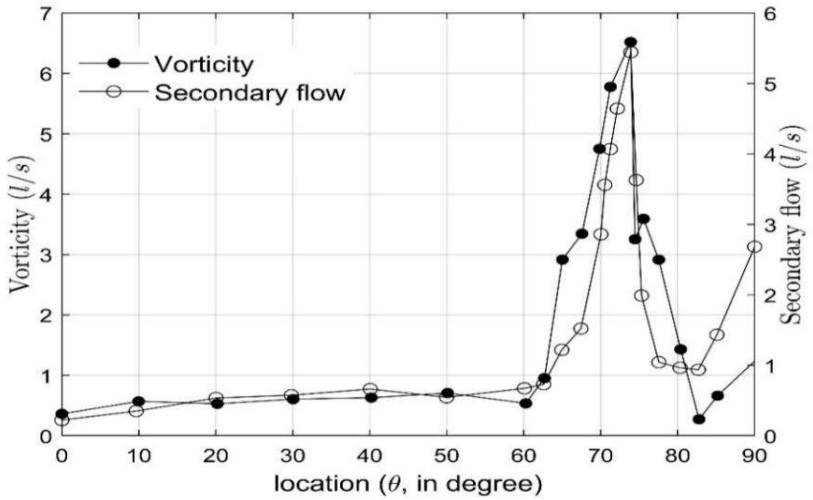

Figure 2.4 Vorticity and secondary flow variation around T-shaped spur dyke located at 75° in 90°bend (Vaghefi et al., 2017a)

Giri et al., (2003) estimated that the flow characteristics near a single straight spur dyke and a group of straight dykes located in a moderately meandering channel having a width to depth ratio nearly equal to 10. They noticed that the bent flow does not properly develop due to small bend angle and magnitude, which was not an important concern as the fully developed condition is not critical for design purposes (Odgaard et al., 1988). It was observed that, although the vertical velocity profiles of flow away from the vicinity of a dyke and back-flow region follow the logarithmic distribution, only a few values near the channel bed followed Prandtl's velocity log-law. They observed that their allocation influences the flow construction around spur dykes on the meandering channel.

2.3 Factors affecting the scour around a spur dyke located in the bend

Scouring is defined as the erosion of sediment materials from the channel bed and banks caused by flow action. Generally, the scour is categorized into the three types such as general scour, constriction scours, and local scour. The scour occurring in the absence of structures such as abutment, pier, spur dyke, etc., are called general or common scour. However, the scour that occurs due to the narrowing of the channel caused by training structures like dykes, J-hook vanes, etc., is known as constriction scour. The protrusion of such structures causes a significant change to flow patterns, and bed configurations in specific reach of the channel which cause excessive scouring around the structure. Such scour is localized around the structure and hence, known as local scour. Generally, the constriction and local scours are merged (Zhang, and Nakagawa, 2008). The scour is sometimes beneficial for environmental aspects. For instance, J-hook vanes are often constructed to promote local scour and to improve morphological diversities in the region (Pagliara et al., 2015). Chabert et al., (1956) categorized the local scour based on channel bed conditions such as live bed and clear water scour. The clear water bed scours are defined as scouring, which occurs when no bed material or sediment transports from

upstream of the scour area to its downstream flow. In such condition, the critical velocity ratio or flow intensity of V/V_c<1 (is less than one) here V is approach velocity and V_c is bed particle critical velocity. In terms of bed shear stress (τ) or velocity (V_*), the clear-water condition occurs when V_*/V_{*c}< 1 where V_{*c} is the critical shear velocity. In contrast, under live bed conditions, the upstream's bed surface material or sediment gets eroded and transported downstream. At this condition, the critical velocity ratio or flow intensity of V/V_c >1 (is higher than one). The variation in average scour depth, and shear velocity is shown in Figure 2.5.

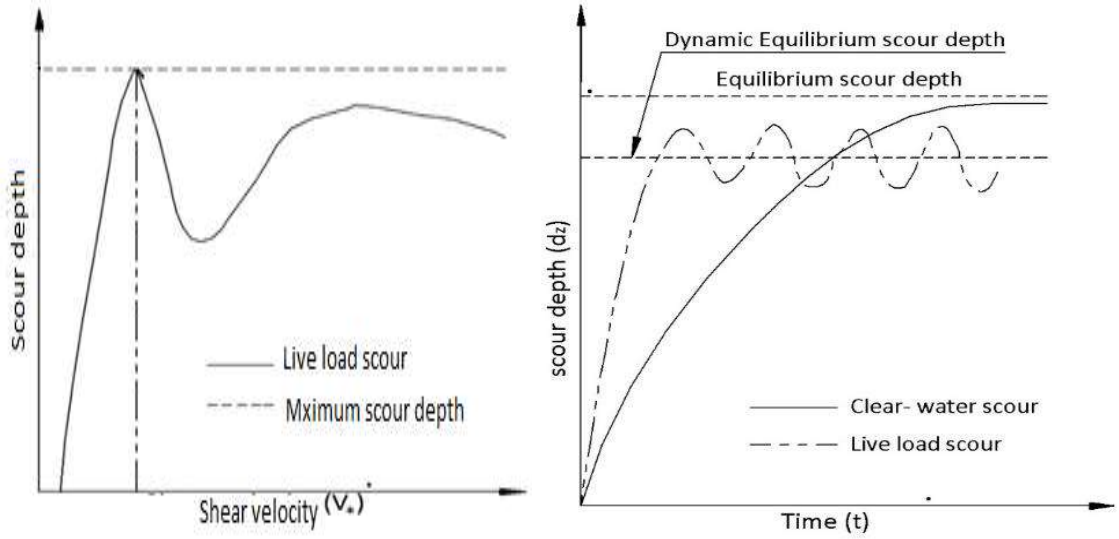

(a) (b)

Figure 2.5 (a) Scour depth variation with shear velocity (V∗), and (b) time (Pandey et al. 2015)

The temporal variation of the scour depth under clear water condition gradually reaches to its maximum value after some time. In live-bed conditions, the scour is gradually increased at the beginning but later it gets fluctuated. This condition is termed the equilibrium scour depth (Chiew, 1984). The condition of the fluctuation was caused due to refilling of the scour hole because of the sediment transport from upstream and, at the same time, escalated vortex eroding the bed particle from the scour hole. Laursen et al., (1953) reported there is no effect of approaching flow conditions on scouring in the

vicinity of bridge piers and abutments under live-bed conditions. According to Pandey et al., (2018) the maximum scour depth under clear-water condition is approximately 10% higher than under live-bed conditions for a particular type of bed material and obstacle.

In general, the scour depth (temporal as well as maximum) around the spur dyke depends on several factors. These factors are listed below:

1. Properties of bed sediment (median diameter and standard deviation of sediment size, mass density, angle of repose, and its cohesiveness characteristics).
2. Properties of flowing fluid (fluid density, kinematic viscosity, gravitational acceleration, and temperature).
3. Approach flow condition (approach flow depth and mean velocity in the form of Froude number and Densimetric Froude number, flow intensity ratio).
4. The geometry of spur dyke (shape, size, and angle of inclination to approach flow).
5. The geometry of the channel (shape of the cross-section, width, and slope of the channel).
6. Time of scouring.
7. Other factors include permeability and submergence of spur dyke.

For spur dyke located in the straight channel, the factors mentioned above are discussed in detail by (Pandey et al., 2018; Zhang, and Nakagawa, 2008). In the spur dyke located in a channel bend, other factors (along with the factors listed above) that influence the scour depth include the location of spur dyke in the channel bend and central radius and angle of bend. To the authors best knowledge, the research on the study of scour around the spur dyke located in a channel bend is very limited and includes few influencing factors such as the geometry of spur dyke and channel and approach flow condition.

The influencing parameters related to the geometry of the spur dyke include its length and wing length. Ghodsian et al., (2009) conducted an experimental investigation on scouring around T-shaped spur dyke located in 90° bend and reported that the maximum scours depth increases with the increase in L/W, and the decrease in B/L where W is the width of the channel, and L and B are length (or effective length in case spur dyke is inclined to the flow direction) and wing length of the spur dyke respectively. A similar result was also reported by other authors irrespective of the type of spur dyke and angle of channel bend (Fazli et al., 2008; Masjedi et al., 2010a, 2011; Vaghefi et al., 2012). The variation of maximum scours depth with L/W, and B/L is shown in Figure 2.6, and 2.7 respectively.

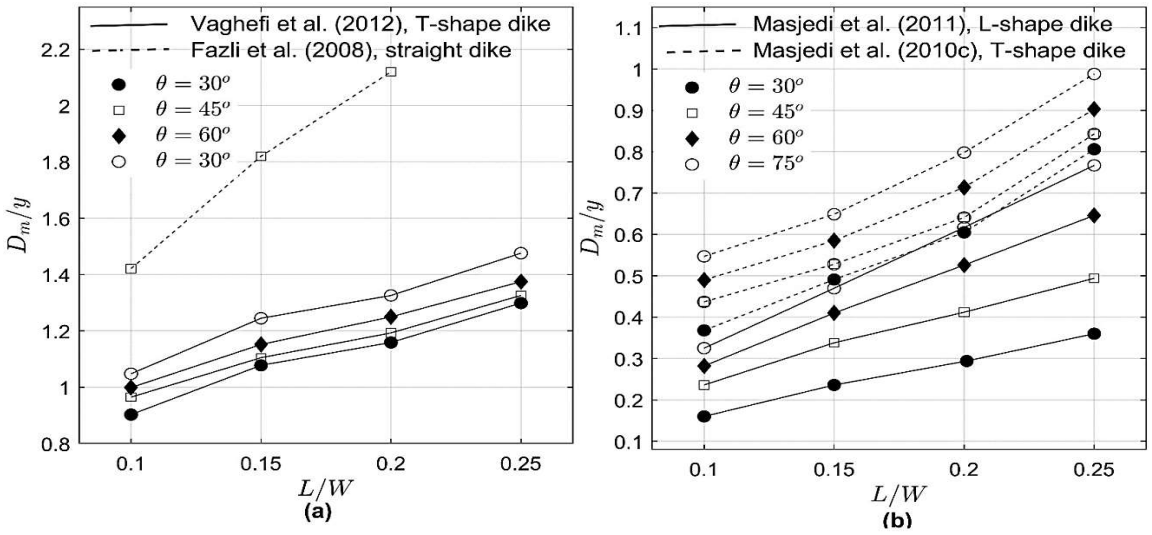

Figure 2.6 Variation of D_m/y with L/W in (a) 90° bend; (b)180° bend

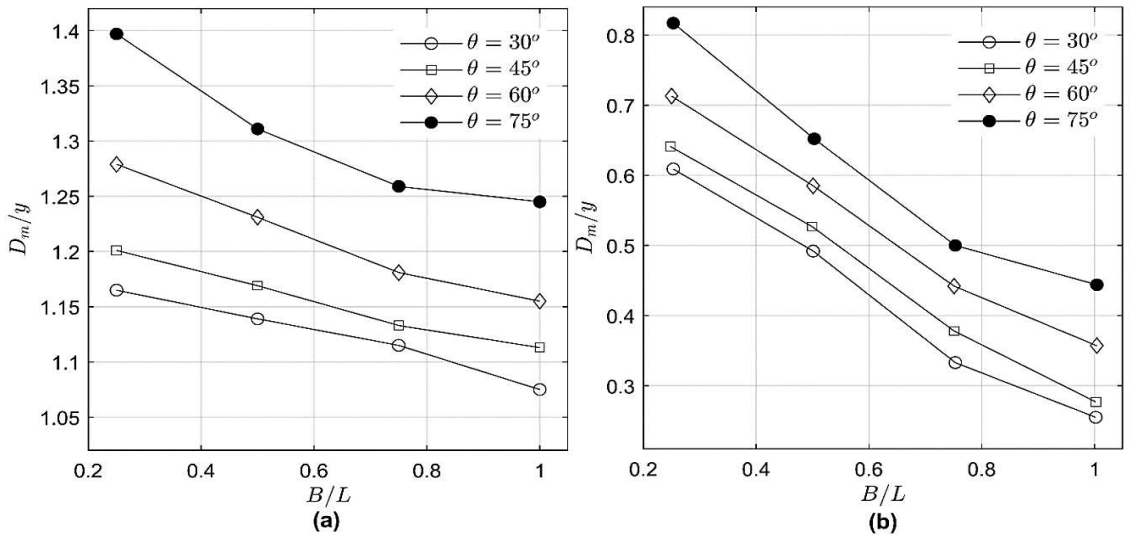

Figure 2.7 Variation of D_m/y with B/L for T-shaped spur dyke located in (a) 90° bend (Vaghefi et al., 2012); (b) 180° bend (Masjedi et al., 2010c)

The width and radius of channel bend are two significant features regarding the geometry of the channel because of an effect on the local scours near the spur dyke. For T-shaped spur dyke localized at a 90°channel, concludes that the decrease in maximum scour depth with increasing R_c/W where R_c is the centre radius of bend shown in Figure 2.8

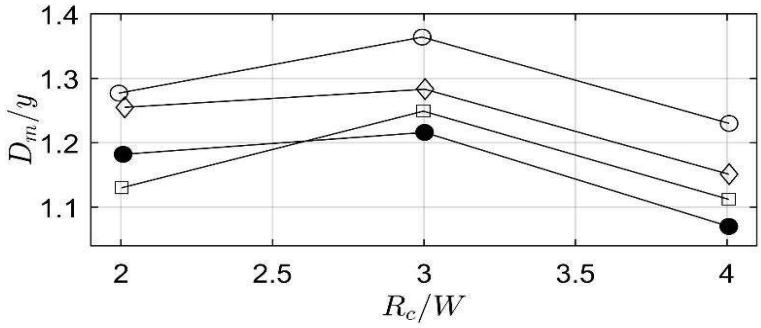

Figure 2.8 Variation of D_m/y with $\boldsymbol{R_c/W}$ for T-shaped spur dyke in a 90° bend, Fr = 0.47, L/W = 0.15 (Vaghefi et al., 2012)

An increase in approach velocity or discharge is associated with increasing Froude number. The variability in the maximum scour depth with Froude number gives a regular manner irrespective of spur dyke and channel bend. Fazli et al., (2008) discussed that the

depth of the scour hole could high up as the discharge get increased. A similar observation was also mentioned in Rashedipoor et al., (2012) shown in Figure 2.9.

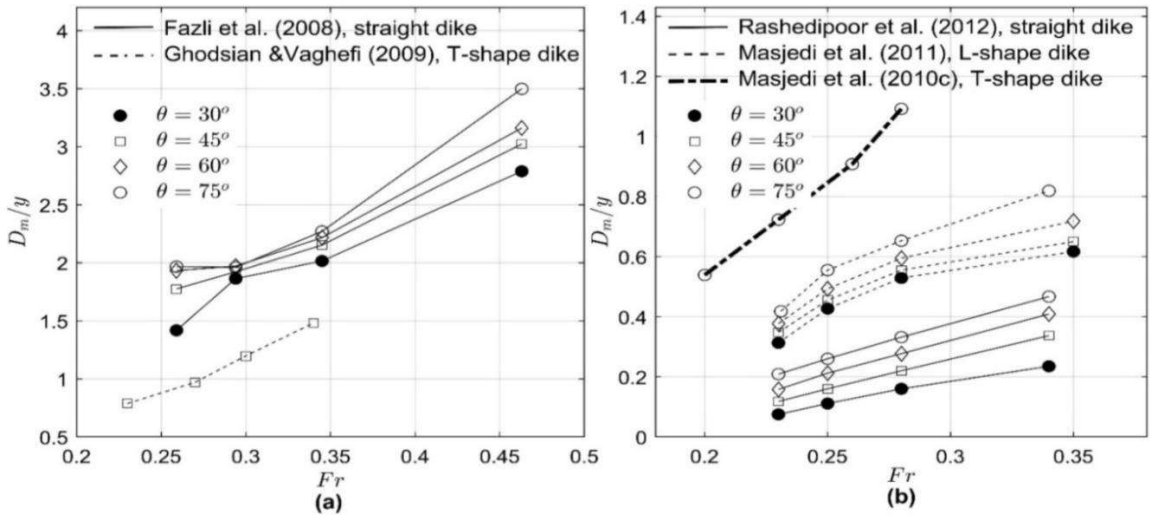

Figure 2.9 Variation of D_m/y with Fr in (a) 90° bends; (b) 180° bends

The increase in maximum scours depth with increasing Froude number for both 90° and 180° channel bends. The above discussions are primarily focused on scour depth (or maximum scour depth). Various researchers have also investigated the other geometric parameters (or dimensions) related to scour holes. The other scour parameters include the downstream length (d), upstream length (c), width (a), and scour volume (V_0), for the T-shaped spur dyke placed in 90° bends, scour dimensions increase with the increase in $\frac{L}{W}$ ratio and Froude number, it decreases with increase in $\frac{B}{L}$. For the T-shaped spur dyke located in a 90° channel bend, the variation of scour geometry with L/W, B/L, and Froude number is shown in Figure 2.10 and Figure 2.11a, respectively. Rashedipoor et al., (2012) estimated that the scour width (a) and total length ($c + d$) increase by increasing the Froude number (Fr), and position of the dyke from the entry to bend (θ) shown in Figure 2.12.

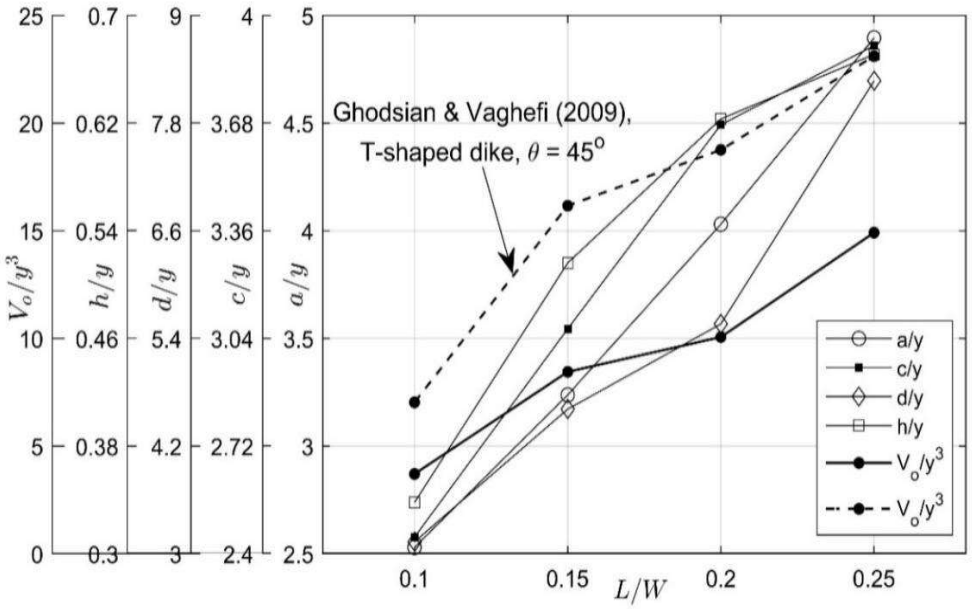

Figure 2.10 Variation of scouring parameters with L/W for T-shaped spur dyke in 90° bend, Fr = 0.33, θ = 45° (Ghodsian et al., 2009)

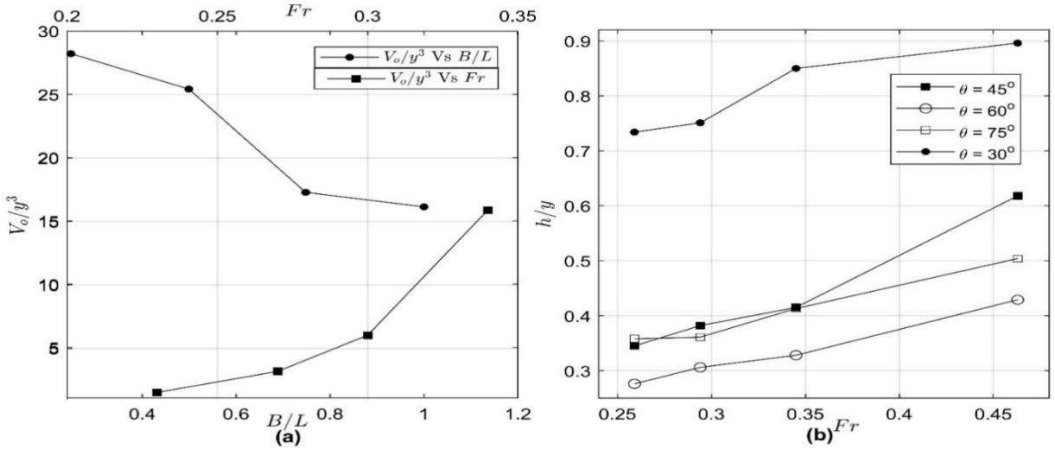

Figure 2.11 Variation of (a) V_o/y^3 with B/L and Fr for T-shaped dyke, θ = 75°(Ghodsian et al., 2009), (b) h/y with Fr for straight dyke (Fazli et al., 2008) in 90° bend

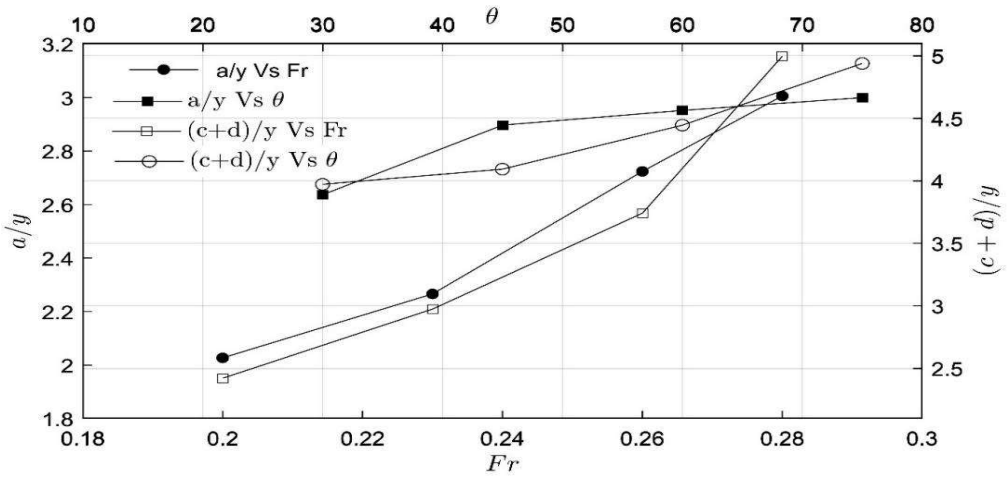

Figure 2.12 Variation of total length (c+d) and width (a) of scour with Fr and θ for straight dyke in 180° channel bend (Rashedipoor et al., 2012)

2.4 Empirical formulation of scour around single spur Dyke

As stated earlier, the scour depth is associated with temporal variation and maximum (or equilibrium) depth. Researchers such as Rouse (1965); Bresuers (1963,1967); (Kohli et al., 2001) asserted that scour process is a ceaseless increment and, therefore, affirmed in the non-existence of an actual equilibrium scour depth. And researchers such as Laursen (1952); Gill (1972); Zaghloul (1983); had an opposite affirmation. Various formulations or empirical relations to predict the equilibrium scour depth are available in the literature. The formulation for maximum scour depth around the spur dyke present on the straight channel is categorized into regime approach, the empirical approach based on the laboratory experiments, and semi-empirical and analytical method. A recent review of Pandey et al., (2018) has summarized these equations, especially for a single or group of spur dyke placed in a straight channel. Many researchers used dimensional analysis for formulating and predicting the scour depth. Fazli et al., (2008) discuss the flow field, local scour near the 90° straight channel of spur dyke. Stabilized the correlation with the maximum scour depth. Another parameter like Froude number channel width, length, and position of dyke and then formulates the empirical equation given below.

$$\frac{D_m}{y} = K_\theta \cdot K_{Fr} \cdot K_L \tag{2.1}$$

Where K_θ, K_L and K_{Fr} are the functions of θ, Fr, and L, respectively. Here, θ = location of spur dyke, D_m = maximum scour depth, and Fr is the Froude number of approach flow conditions given by $V/\sqrt{gy}$, where$y$ = approach flow depth and g is the acceleration because of gravity. The coefficients in Equation (2.1) are related to scour parameters as;

$$K_\theta = a_1 \cdot ln\theta + a_2 \tag{2.2}$$

$$K_{Fr} = e^{a_3 \cdot Fr} \tag{2.3}$$

$$K_L = (L/W)^{a_4} \tag{2.4}$$

Where, a_1, a_2, a_3, and a_4 are constants, equal to 0.94, 4.6, 2.86 and 0.45 respectively.

Masjedi et al., (2010b) worked at T- shape spur dyke at 45^0, 60^0, and 180^0 angle bend and established an empirical relation between maximum scour depth and location and Froude number given by;

$$\frac{D_m}{y} = 25.3\,[Fr]^{1.7}\left[\frac{\theta}{180}\right]^{0.13} \tag{2.5}$$

At 60^0 straight spur dyke in 180° bend angle of the channel, Masjedi et al., (2010a) used the general form of the empirical equation for temporal scour depth variation given by Coleman et al., (2013) and modified the constants involved in the equation to fit the data, represented by Equation (2.6). It was seems that the temporal and maximum depth of scour can increase with the increase of V_*/V_{*c}.

$$\frac{d_z}{\sqrt{Ly}} = 0.53\left[\frac{V_*}{V_{*c}}\right]^{0.55} ln\left[\frac{tV_*}{\sqrt{Ly}}\right]^{0.53} \tag{2.6}$$

Where d_z = scour depth at any time instant t. To obtain the maximum scour depth $d_z = D_m$, t in Equation (2.6) is replaced by t_e. Here, t_e is the time required to reach equilibrium for maximum scour depth. It is interesting to note that Equation (2.6) represent the dependency of scour depth on t_e, i.e., the time duration for which the experiment runs. For a given approach flow condition, the duration for which an experiment runs is usually lesser than the time required for a scour hole to develop its full-length depth (Kothyari et al., 2001). Masjedi et al., (2010c) experimented with studying the temporal development of scour depth around a T-shaped spur dyke located in a 180° channel bend and developed an empirical equation based on dimensional analysis, given by;

$$\frac{d_z}{y} = 1.25\,[Fr]^{0.5}\left[\frac{\theta}{180}\right]^{0.25}\left[\frac{L}{W}\right]^{0.25}\left[\frac{B}{L}\right]^{0.05} ln\left[\frac{t+t_e}{t_e}\right]^{0.45} \tag{2.7}$$

The maximum scour depth, D_m is reached at $t = t_e$, and can be computed using Equation (2.7) as;

$$\frac{D_m}{y} = 0.39\,[Fr]^{0.5}\left[\frac{\theta}{180}\right]^{0.25}\left[\frac{L}{W}\right]^{0.25}\left[\frac{B}{L}\right]^{0.05} \tag{2.8}$$

Similarly, to study the scour around L-shaped spur dyke located at 180^0 flume bend and developed an empirical equation for temporal scour variation given by Equation (2.9) (Masjedi et al., 2011). The empirical equation was developed using dimensional analysis and is related to scour parameters as;

$$\frac{D_m}{y} = 6.15\,[Fr]^{1.12}\left[\frac{\theta}{180}\right]^{0.5}\left[\frac{L}{W}\right]^{0.28} ln\left[\frac{t+t_e}{t_e}\right]^{0.22} \tag{2.9}$$

For the above equation the influence of the wing length of spur dyke on scour depth was neglected. For maximum scour depth, D_m reached $t = t_e$ Equation (2.9) can be reduced to;

$$\frac{D_m}{y} = 0.938\,[Fr]^{1.12}\left[\frac{\theta}{180}\right]^{0.5}\left[\frac{L}{W}\right]^{0.28} \tag{2.10}$$

The geometry of scour hole near T-shape spur dyke at 90° bend, formulated an empirical equation to obtained the maximum dimension of scour parameters using dimensional analysis expressed as;

$$\frac{\varphi}{y} = k_1\left[\frac{B}{L}\right]^{k_2}\left[\frac{\theta}{90}\right]^{k_3}\left[\frac{R_c}{W}\right]^{k_4}\left[\frac{L}{W}\right]^{k_5}\left[\frac{V}{V_c}\right]^{k_6} \tag{2.11}$$

Where φ = maximum dimension of the scour parameters, and k_i where i =1, 2, 3, 4, 5, and 6 are constants, listed in Table 2.1. The importance of each parameter on the scour is, in descending order as V/V_c, L/W, R_c/W and $\theta/90°$. It should be noted that Equation (2.11) is valid for the ranges $0.25< B/L <1$; $0.7 < V/V_c <0.98$; $2< R_c/W < 4$; $0.1 < L/W <0.25$; and $L/d_{50} >70$, where d_{50} is the median diameter of bed sediment (Vaghefi et al., 2012).

Table 2.1 Value of constants in Equation 2.11

Scour parameter	k_1	k_2	k_3	k_4	k_5	k_6
D_m	4.1	-0.11	0.13	-0.1	0.54	2.36
a	14.02	----------	0.183	-0.1	0.554	2.626
c	6.51	----------	0.178	0.288	0.455	2.023
d	122.4	-0.45	0.19	-1.2	0.43	10

An attempt was made to validate the extent of applicability of the empirical equation proposed by various researchers with experimental data (observed value), as shown in Figure 2.13-2.17.

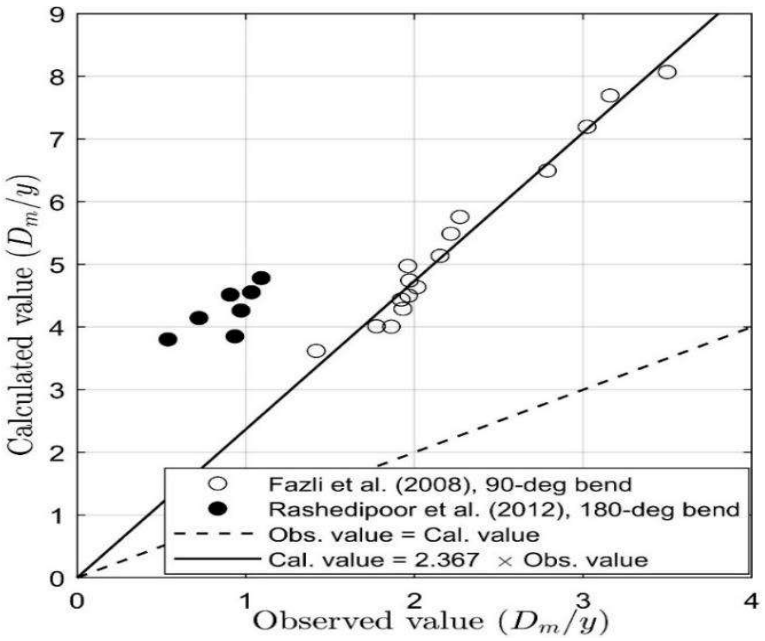

Figure 2.13 Comparison of the observed value of maximum scour depth with Equation (2.1) by (Fazli et al., 2008)

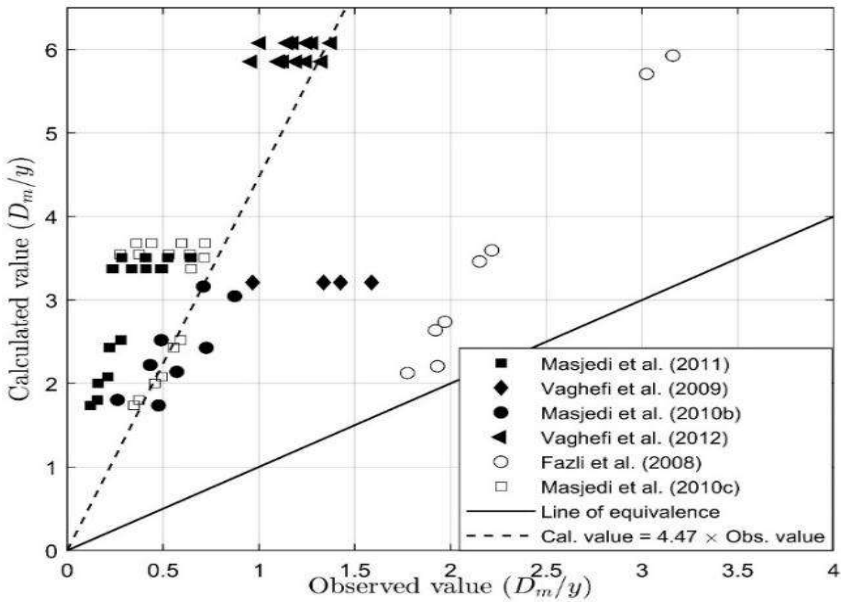

Figure 2.14 Comparison of the observed value of maximum scour depth with Equation (2.3) (Masjedi et al., 2010b)

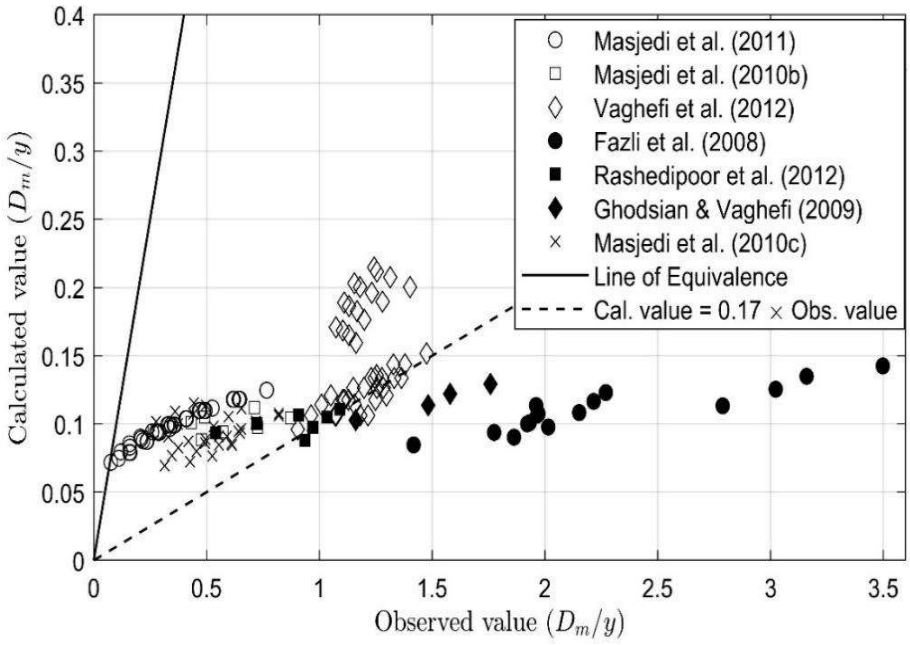

Figure 2.15 Comparison of the observed value of maximum scour depth with Equation (2.8) by (Masjedi et al., 2010c)

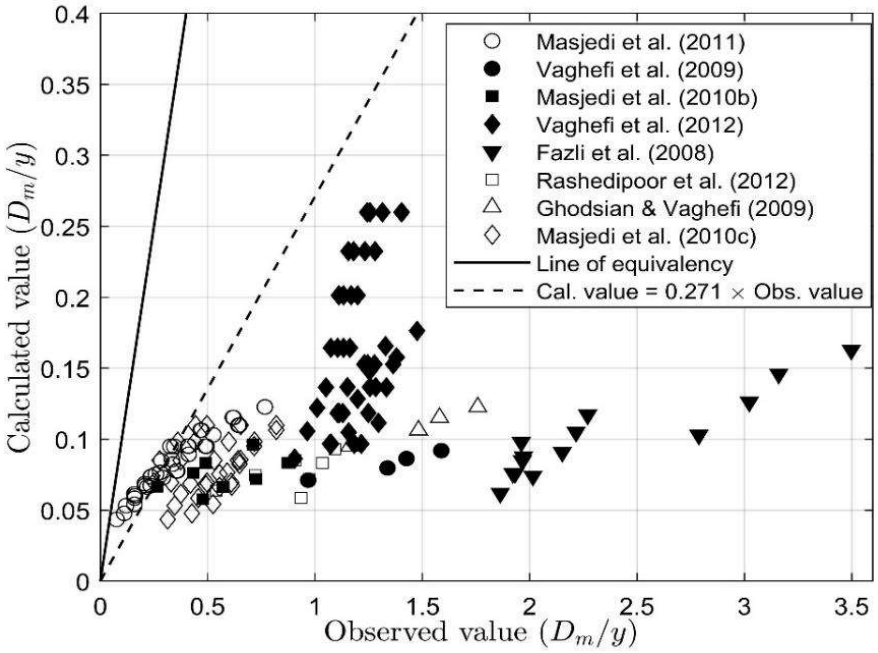

Figure 2.16 Comparison of the observed value of maximum scour depth with Equation (2.10) (Masjedi et al., 2011)

The equation developed for a T-shaped or L-shaped spur dyke can be applied on the straight spur dyke by keeping the value of B/L equal to 1, to eliminate the influence of the wing length ratio. Similarly, equations applicable to the spur dyke located in a 90°

bend can be applied to the one located in a 180^0 bend or vice-versa. It has been observed that the equations are different for different type of channel bend and spur dyke. It is noted that the equations do not fit well with the experimental data recorded by their respective researchers, i.e., the data points deviate significantly from the line of equivalency. From Figure 2.15 and 2.18, it is shown that the calculated value obtained using equations given by Fazli et al., (2008); Masjedi et al., (2010b, 2010c, 2011) was approximately 2.36, 4.47, 0.17, and 0.271 (average) times the corresponding experimental data, respectively. Generally this type of error occurs in either observation during experiments or data analysis, or both, and some time due to limited limited set of experimental data to develop the empirical equations. Therefore, suggested to avoid Equation (2.1-2.10) Figure 2.19, Equation (2.11) given by Vaghefi et al., (2012) shows a good correlation with the corresponding experimental data. Still, its application is limited to the T-shaped spur dyke placed in a 90° channel bend. A more detailed experimental research, including various influencing parameters and data analysis, is required to develop empirical equations.

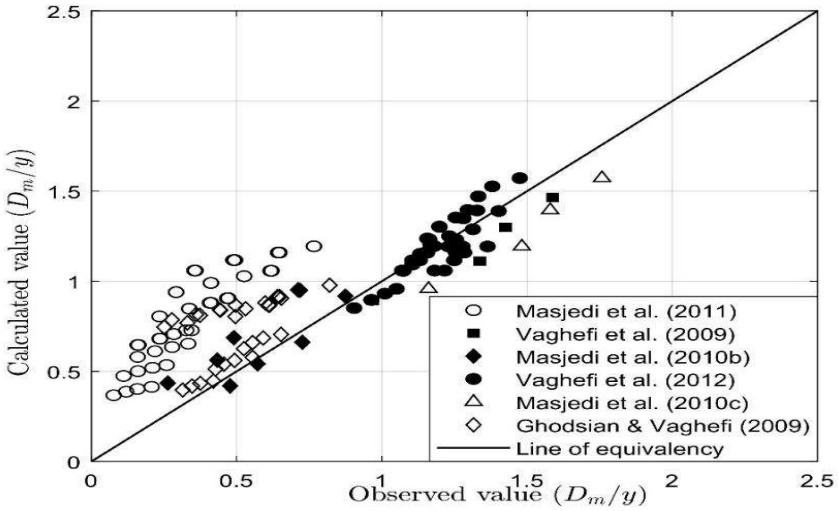

Figure 2.17 Comparison of the observed value of maximum scour depth with Equation (2.11) by (Vaghefi et al., 2012)

The majority of research work in this regard has been carried out in the flume, leading to several empirical formulae, which are data-driven and curve fitting. Further, such formulation is scale-dependent, which makes it less resilient for real-life engineering applications. No field experiment has been done to the best knowledge related to the scour around the spur dyke located in a curved channel. This shortcoming of existing researches has been raised by Manes, and Brocchini, (2015). The turbulence (PTT) phenomenological theory to study the scour field around cylindrical elements placed in a straight channel. Developed an analytical equation for maximum scour depth assessment, which is scale-independent and physically driven. Some authors have further extended the PTT theory to study local scour around the different structures (Coscarella et al., 2020; Zhou et al., 2020). However, the PTT theory has not been yet attempted to study the scour around the spur dyke located in a bend. It can be treated as the future scope of the study.

2.5 Bed topography around the spur dyke

The flow characteristic in the channel bend significantly affects bed topography. The inclusion of a spur dyke in between the flow further adds complicacy to it. The development of scour holes near a spur dyke placed in a bend occurs due to complex flow formed due to the interaction between the cross-current flows and vortices formed around the structure (Pandey et al., 2018). The bed topography, in general, is characterized by sediment scission at the outer edge and deposition at the inner edge, which is illustrated in Figure 2.18a.

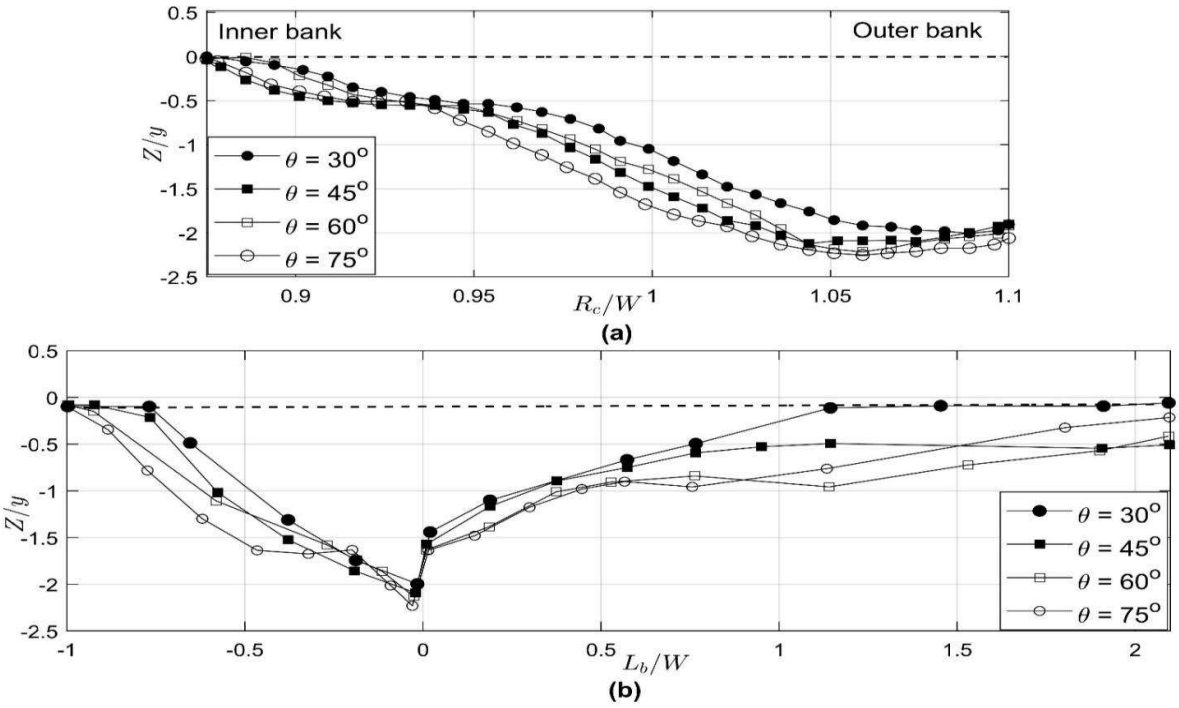

Figure 2.18 (a) Lateral and (b) longitudinal bed profile for a straight spur dyke located at θ = 45° in a 90°channel bend (Fazli et al., 2008)

Sedimentation on the inner edge is caused by the lateral migration of eroded bed material due to secondary flow and cross-current. The sediment gradually shifts downstream and formation of ridges occurs. The position of spur dyke towards the exit of bend, the influence of secondary flow gradually diminishes.

Hence, the two processes get interchanged, i.e., erosion and sediment deposition occurs at both inner and outer edges, respectively (Fazli et al., 2008). The scour holes are characterized by ridges just downstream of the spur dyke. The sediments then eventually get transported further to form smaller ridges downstream. The lateral and longitudinal bed profile at the position of spur dyke is illustrated in Figure 2.20b. For the T-shaped spur dyke at 90° bend, Ghodsian et al., (2009) reported that the downstream scour holes and ridges move up to a distance of 7 to 14 times the approach flow depth. A narrow degradation zone formation, which travels from the stagnation zone upstream of spur

dyke that goes downstream in an inclined way. The bed topography shows some typical and distinct features for different allocations of a dyke in a river bed.

Fazli et al. (2008) estimated that the maximum local scour hole is present at mid-length upstream straight channel spur dyke. For a T-shaped spur dyke at 90° bend, a formation of 2 main local scour holes; one hole located upstream another on the inner edge of the dyke, and the distance between these two was approx 10-20% of spur dyke length. The depth of scour at downstream increases with increase in B/L, and its distance from spur dyke increases with the increase in B/L up to 0.75 and then decreases (Vaghefi et al., 2012). The spur dyke present at an azimuthal angle of 60° and 75°, the scour shifts near the inner edge up to the exit of bend. The scour dimensions of the dyke situated at 90° channel bend can broaden to the inner edge when the length is approximately 20% percent of channel width, i.e., L/W = 0.20 Fazli et al., (2008); Ghodsian et al., (2009);

Biswas et al., (2015), while studied scour in the bend of a trapezoidal channel with no allocation of training structure, found that around 30° azimuthal section the maximum scour and bed sedimentation occur near most of the outer and inner edge or bank respectively. For azimuthal sections of 0° (entry to bend) and 70° (exit from bend), they noticed that little scour is also found on the inner bank caused by cross-current from the outer bank.

They further reported increasing the depth at the outer bank with the increase in azimuthal sectional angle, with maximum occurring near 30° and then keep on decreasing. The T-shaped spur dyke located near the entry of 90° channel bend, i.e., θ = 30° and 45° the significant formation of ridges at the downstream. In spur dyke located near the exit, i.e., θ = 60° and 75°, the eroded bed material transports to the straight portion of the channel.

It results in a more or less uniform distribution of sediment along the width of the channel, causing insignificant ridge formation shown in Figure 2.19.

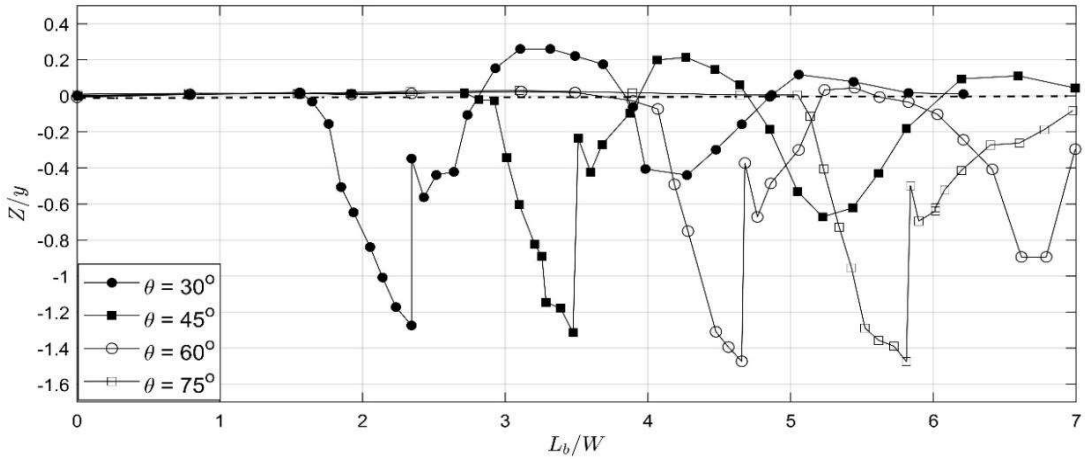

Figure 2.19 Longitudinal bed profile variation for a T-shaped spur dyke located in the 90° channel bend (Vaghefi et al., 2012)

For the straight spur dyke at 90° bends, the ridge height decreases up to the azimuthal angle of 60° and then increases for a constant value of Froude number as shown in Figure 2.11b. The bed topography at downstream of the T-shaped spur dyke is that the maximum height and number of ridges increase with an increase of spur dyke length. And the flow over the ridges generates vertical vortices, which then strike the channel bed downstream, resulting scour formation.

2.6 Numerical investigation of flow and scour process around spur dyke in bend

Earlier, the conventional methods used to evaluate the scour processes involve empirical formulas, graphs, etc. These methods become less reliable when an in-depth assessment is required. The recent development in numerical modeling such as CFD (Computation Fluid Dynamics) has become more reliable. Zhang, and Nakagawa, (2008) reviewed past literature related to the numerical investigation of flow characteristics, sediment transport, bed deformations, and so on in a channel with or without any structure. Classification of

the numerical modeling of researches related to scour processes in terms of adopted channel bed features are as (1) planar or unscoured bed; (2) scoured bed; (3) deformed and movable bed. Furthermore, briefly discussed the types of numerical models being widely used in the related area of research, such as the Turbulence Flow Model, Large Eddy Simulation (LES), and so on.

Chen et al., (1989) simulated the flow field and turbulent kinetic energy distribution in a channel using a depth-averaged 2D flow model and $k-\varepsilon$ equations. Tingsanchali et al., (1990) also worked on a similar model to predict bed shear stress in the stream channel. Mayerle et al., (1995); Zhou (2001), used a static pressure model and LES model, respectively, for studying flow field near around the dyke in a straight channel. Peng (2004), validate the mathematical model and investigated the characteristics of scour around a single spur Dyke. Xuelin et al., (2006) implemented the LES model to investigate the 3D flow pattern and vortex around a non-submerged spur dyke. Versteeg et al., (2007) implemented the Finite Volume Method (FVM) for solving Navier-Stoke Equation and other related to it. When these equations are validated using the experimental data, show the good fit. Yazdi et al., (2010) applied the Volume of Fluid (VOF) method and solved a fully 3D model to simulate free-surface flow around a spur dyke. They investigated the effect of parameters such as angle and length of spur dyke approaching flow discharge on flow characteristics and bed shear stress. They reported that the model showed a good fit when validated against the observed data. In the 1990s, it was challenging to simulate fine sediment in the physical model and other applications such as simulating sediment filling in reservoirs or channels. Therefore, Oslen (2018), and colleagues began to develop the SSIIM model (Sediment Simulation in Intakes with a Multiblock Option), and it is still under improvement. The SSIIM model solves the Navier-Stokes equations with $k-\varepsilon$ equations on a three-dimensional, non-orthogonal

grid. By default, it uses a semi-implicit method to calculate the pressure term Oslen (1999), for equations involving pressure (simple method). Solomatine, and Otsfeld, (2012) used this model to study (numerically probe) the flow and scour features around a T-shaped spur dyke placed in a 90° bend. Therefore, its consequences are discussed in subsequent paragraphs. For other cases, if any, the same is mentioned.

The flow characteristics near spur dyke in a channel bend are numerically studied concerning parameters like Froude number of flow condition, submergence ratio of the structure, relative curvature of the bend, and separation between two successive spur dyke. According to Vaghefi et al., (2017b) the effect of Froude number and submergence ratio on turbulence flow characteristics around the dyke in a channel bend with moving bed. Generally, it was found that, by increasing submergence ratio, percentage and range of kinetic energy reduced near the wing of a dyke, and eddy viscosity closed to bed increases. The dimensions of the separation zone decrease with the increase in spur dyke submergence ratio and the relative curvature of the bend affirmed that with increasing spur dyke submergence ratio, the dimensions of the separation zone decrease. With an increase in the spacing between two spur dykes present at the bend, the span of the separation zone upstream of the first spur dyke remains nearly constant, but the length of the separation zone rises to 8.1 times the length of the spur dyke at downstream. The change in flow separation and reattachment zones causes the change in the dimensions of vortices around the dyke. The power of secondary flow downstream is more significant than upstream of the dyke and it reduced to 31% (Vaghefi et al., 2016, 2015). Literatures suggest that stream wise velocity is increased near the bed because of downward seepage. In recent studies Deshpande, and Kumar, (2016); Patel et al. (2015), the effect of downward seepage through porous boundaries is clearly visible on the time averaged turbulent characteristics of flow.

The component around the dyke observed that transverse velocity get rises from the inner bank to the dyke present then gets reduced to the outer bank. They further affirmed that the transverse velocity does not change significantly with the increase in submergence of the dyke. In a submerged dyke, the longitudinal flow component could also increase with increasing submergence. RNG $k-\varepsilon$ turbulence model (other than the SSIIM model)solved using FVM to simulate the flow field near the spur dyke on the river bend and found that the critical velocity and Froude number increase simultaneously.

The relative effect of curvature on scouring formation near the spur dyke showed that maximum scours were found at the upstream head of the construction. With an increase in relative curvature, the scour depth increases and it decreases with the increase in submergence ratio. The height of the ridge (sediment deposition) increases simultaneously as the relative curvature of the bend increased the submergence ratio forming a second hole downstream in a 25% dyke submergence ratio (Randan and Vaghefi, 2016; Vaghefi et al., 2014, 2016).

2.7 Gene Expression Programming

Generally, field experiments in theoretical hydraulics are beyond the scientific extent and, scope of hydraulics and river engineering. In these fields, the experimental work needs more space and money. The progress of computational hydraulics depends on the theoretical aspects of the hydraulics field. This condition can limit the progress occurred in this field. On the other hand, the parameter used in hydraulics was better defined by the use of evolutionary algorithms such as genetic algorithm, genetic programming, and gene-expression programming, commonly known as soft computing techniques. These techniques are much simple for their simplicity and received much attention from a scientist in any field of science and engineering (Guven and Gunal, 2008a; Azamathulla et al. 2010; Azamathulla and Zahiri, 2012; Guven and Azamathulla 2012; Azamathulla

and Jarrett, 2013; Najafzadeh et al., 2013; Onen 2014). The main aim of the soft computing technique is to overcome difficulties in the real world, especially in the field of engineering (Gandomi and Alavi, 2011, 2021). Guven and Azamathulla, (2012) the following equation was developed for estimation of maximum scour depth (d_s), width (d_w), and location (l_s) at the downstream of the flip bucket spillway by using GEP, respectively

$$\frac{d_s}{d_w} = \left[\frac{d_{50} + q}{\emptyset} - (H_1 - q - 1.199)\left(5.616\frac{d_{50}}{\emptyset}\right)\right] \times [0.309\emptyset(R + (d_{50} + 0.185)(H_1 d_{50}))^{-0.5}] \quad (2.12)$$

$$\frac{w_s}{d_w} = \left[\frac{q - 0.006^{d50} + 1.168^{R+H_1}}{2.336\emptyset}\right]^{0.5} \left[\frac{7.521d_{50} + 3.955H_1 - 2_q}{0.428\emptyset^{-1}} + 15.42\emptyset\right]^{0.5} \quad (2.13)$$

$$\frac{l_s}{d_w} = \left[\frac{e^{\emptyset}}{R}(H_1 - d_{50} + 0.495 + 2.878(q)^{-1}\right][R(q + H_1 - 9.948d_{50})^{-0.5}(2H_1 + q + \emptyset)] \quad (2.14)$$

In which q = unit discharge over the spillway, H_1= total head, R = radius of the bucket, $\emptyset$ = lip angle of the bucket, d_w = tail water depth, d_{50} = median grain size, and g = acceleration due to gravity.

The result of above GEP equations are compared with regression equation and neural networks approach. The comparison revealed that the GEP models (Eq. 2.12–2.13) have higher accuracy to estimate the scour depth.

$$\frac{d_s}{Y} = \frac{b}{Y}\left[0.595 - Fr - \left(\frac{d_{50}}{Y}\frac{b}{Y}\right)^2\right] + Fr\left(Fr + 0.063 - \frac{d_{50}}{Y}\right) - \left(\frac{d_{50}}{Y}\right)^2(\sigma - 1) + Fr\,\frac{b}{Y}\left(Fr - \frac{3.24d_{50}}{Y(Fr-1)}\right) \quad (2.15)$$

Here Y = approach flow depth, Fr = Froude number, b = pier width and ¢ = standard deviation of particle grain size distribution.

Using the GEP model, estimate the pier scour depth with the help of Eq. 2.16. In this experiment 4 main dimensionless parameter like pier width (D/d_{50}), approaching flow depth (Y/d_{50}), threshold flow velocity ($(V_2–Vc_2)/(4gd_{50})$), and pier scour depth (d_s/D) are independent variable in Eq. 2.16.

$$\frac{d_s}{D} = \left[\frac{Y}{\alpha d_{50}}\left(\frac{V^2 - V_C^2}{\Delta g d} / \frac{D}{d_{50}}\right)\right]^{log\left(\frac{D}{d_{50}}, \frac{\Delta g d}{V^2 - V_C^2}\right)} \left(\frac{\frac{D}{4.94\, d_{50}}\left(\frac{V^2 - V_C^2}{\Delta g d_{50}}\right)^{2.05}}{\left(\frac{D}{d_{50}}\alpha\right)^{log\left(\frac{D}{1.44\, d_{50}}\right)}}\right)^{0.156} \qquad (2.16)$$

Where D = pier width or diameter, Y = approaching flow depth, V = average approaching flow velocity $\Delta = \left(\rho_s/\rho_w\right) - 1$ is the relative submerged density of sediment which ρ_s and ρ_w are the buoyant sediment density of water density, respectively, and α = channel open-ratio.

Due to the accuracy in the result of the GEP model, the researcher will be more attracted to the soft technique for handling hydraulic parameters (Moussa (2013); Azamathulla and Jarrett, (2013); Jarrett, 1984). Guven and Aytek, (2010) compared GEP with (SRC) and (MLR). Zakaria et al., (2010) used the GEP model to predict total load transport in three rivers, namely, Kurau, Langat, and Muda.

2.8 Summary and Conclusion

The development in researches related to scour around a spur dyke has been significantly increased over the decades. However, the majority of researches is conducted in a straight channel. In comparison, there is still far less development in research related to spur dyke present at the channel bend. The experimental field study on scour near around a dyke located in a channel bend is conducted under the clear-water condition. Ideally, the

maximum scour depth is reached after infinite time, but various researchers reported the observation time up to three-four hours depending on various experimental conditions when the change in bed elevation becomes nearly negligible. In case of live bed condition, the equilibrium scour depth fluctuates between about a mean value. Therefore, the observation time in such a case may extend largely beyond three-four hours. However, it should be noted that the natural phenomena of flow and scour around the structure occur under the live bed condition. Therefore, the experimental study under live bed condition should also be conducted.

The research in this field has been concentrated on a T-shaped spur dyke at 90° channel bend. The minimal focus has been given to other types of bends or curved channels such as 180° bend, meandering channel, sinusoidal channel, and so on. Furthermore, other types of spur dyke like straight, L-shaped, Oblong, and so on are almost neglected. The experimental, as well as the numerical study, should also be carried out for these types of channel bends, and spur dykes. In the case of the 180° bend, the researchers are mainly limited to the experimental study of scour depth observation only. Even so, the empirical equations for maximum scour depth have been developed on a minimal set of experimental data. Therefore, the equations have very limited applications. Hence, a large set of data collected from various pieces of literature can be analysed to obtain a single or a set of formulations, which could have a broader range of applications.